

Early detection of neonatal hypoxic–ischemic white matter injury: an MR diffusion tensor imaging study

Youngseob Seo^{a,b}, Geun-Tae Kim^c and Jin Wook Choi^d

The purpose of this study was to compare diffusion tensor metrics in normal age-matched neonates with survivors of hypoxic–ischemic encephalopathy (HIE) and extracorporeal membrane oxygenation (ECMO). Thirty-five normal, 27 HIE, and 13 ECMO infants underwent MRI at 3 T.

Neurodevelopmental assessments were performed.

Fractional anisotropy (FA), axial diffusivity (AD), and radial diffusivity (RD) of the inferior fronto-occipital fasciculus, inferior longitudinal fasciculus, anterior commissure, genu corpus callosum and splenium of the corpus callosum, anterior and posterior limb of the internal capsule, superior longitudinal fasciculus, and the centrum semiovale were analyzed with tract-based spatial statistics modified for use in neonates. Linear regression analysis was performed, and 95% confidence intervals were created for age effects on the tensor metrics with the control patients. Two-sample *t*-test was done to determine whether there was a difference in the tensor metrics between the normal and patient cohort. There was a statistically significant age effect on the FA and RD in the selected regions of the brain ($F < 0.05$) and a group difference in the FA and RD between the normal and the HIE group ($P < 0.05$). The group difference in the FA and RD between the normal and ECMO groups was seen in the anterior commissure, genu corpus callosum, right inferior

longitudinal fasciculus, fronto-occipital fasciculus, centrum semiovale, and superior longitudinal fasciculus ($P < 0.05$). Patients who were outside the 95% confidence intervals of the FA, AD, and RD overlapped with those with abnormalities clinically and on the conventional MRI. In conclusion, diffusion tensor imaging can play a significant role in detecting infants with early indications of hypoxic–ischemic brain injury. *NeuroReport* 28:845–855
Copyright © 2017 The Author(s). Published by Wolters Kluwer Health, Inc.

NeuroReport 2017, 28:845–855

Keywords: diffusion tensor imaging, extracorporeal membrane oxygenation, hypoxic–ischemic encephalopathy, infant, tract-based spatial statistics

^aCenter for Medical Metrology, Korea Research Institute of Standards and Science, ^bDepartment of Medical Physics, University of Science and Technology, Daejeon, ^cDepartment of Internal Medicine, Kosin University College of Medicine, Busan and ^dDepartment of Radiology, Ajou University School of Medicine, Suwon, Republic of Korea

Correspondence to Youngseob Seo, PhD, Center for Medical Metrology, Korea Research Institute of Standards and Science, 267 Gajeong-Ro, Yuseong-Gu, Daejeon 34113, Republic of Korea
Tel: +82 428 685 479; fax: +82 428 685 058; e-mail: yseo@kriss.re.kr

Received 8 May 2017 Revised 3 June 2017

Introduction

Neonatal cerebral white matter (WM) is vulnerable to a variety of perinatal insults including hypoxic–ischemic encephalopathy (HIE), sepsis, hypotension, hydrocephalus, and prematurity [1,2]. Although the basal ganglia, thalami, hippocampi, and perirolandic gray matter are the areas that are most vulnerable to HIE, the WM is also at risk [3].

Neonatal magnetic resonance imaging (MRI) is widely used to predict outcomes following HIE with injury to the basal ganglia and thalamus and perirolandic regions highly predictive of motor and tone problems with variable cognitive delays in early childhood [4]. Therapeutic hypothermia decreases the frequency and severity of MR abnormalities and improves short-term outcomes [5]. The absence of injury to the central gray nuclei and to watershed regions is associated with normal motor development but does not insure subsequent normal neurocognitive development [6]. Neonatal cerebral WM injury may also be a sequela of

extracorporeal membrane oxygenation (ECMO), which is a modified form of cardiopulmonary bypass used for complications of congenital heart disease (CHD), congenital diaphragmatic hernia (CDH), and severe hypoxic respiratory failure when aggressive measures such as high-frequency ventilation and inhaled nitric oxide fail to maintain adequate oxygenation [7]. In survivors of neonatal CHD supported with ECMO after cardiac surgery, relatively minor signal abnormalities in cerebral WM by MRI may be associated with moderate disabilities in cognitive domains, as demonstrated by the standardized measures of neurodevelopmental assessment [8]. Although ECMO significantly improves survival and decreases disability, 15–50% of survivors of severe hypoxic respiratory failure requiring ECMO have poor neurodevelopmental outcomes, even in the absence of brain injury according to conventional MRI (cMRI) [9].

More advanced MRI techniques have been studied with the intent to improve the sensitivity of MR to WM injury, one being diffusion tensor imaging (DTI). DTI provides information about WM integrity, which cannot be gained with cMRI because of the sensitivity of DTI to alternations in the WM macrostructure that affect the diffusion of water within tissues [10]. Scalar measures derived from

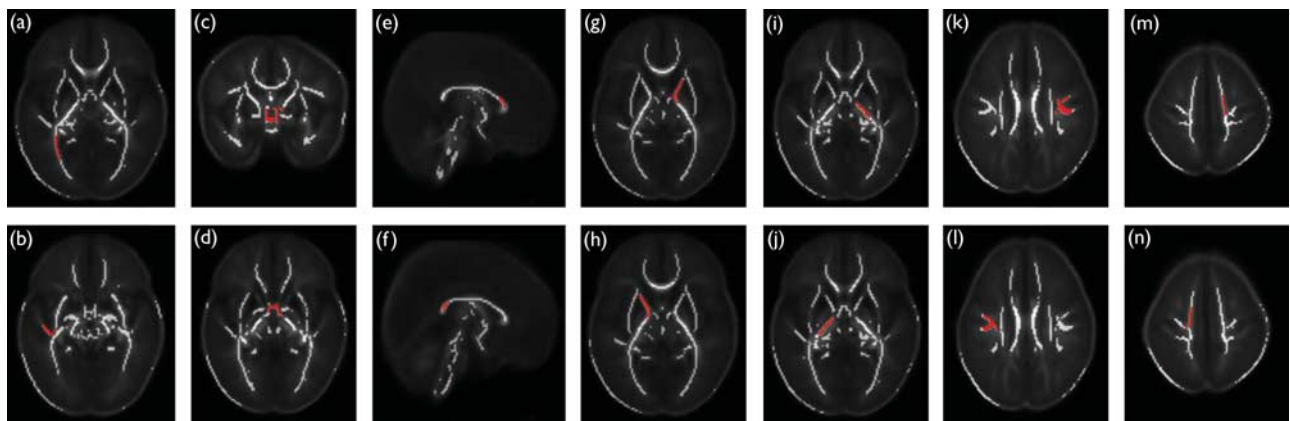
This is an open-access article distributed under the terms of the Creative Commons Attribution-Non Commercial-No Derivatives License 4.0 (CCBY-NC-ND), where it is permissible to download and share the work provided it is properly cited. The work cannot be changed in any way or used commercially without permission from the journal.

Table 1 Baseline characteristics of the infants

	Control group (N=35)	HIE group (N=27)	ECMO group (N=13)	P-value control vs. HIE	P-value control vs. ECMO
Number of boys [n (%)]	22 (63)	14 (52)	7 (54)	0.24	0.13
Birth weight (mean±SD) (g)	3410±412	3404±410	3398±440	0.31	0.18
Length (mean±SD) (cm)	51±3	51±2	50±3	0.45	0.37
Head circumference (mean±SD) (cm)	34.8±2.0	34.6±2.0	35.0±1.9	0.42	0.36
Apgar score <5 [n (%)]					
At 1 min	0 (0)	24 (89)	11 (85)	0.008 [†]	0.01 [†]
At 5 min	0 (0)	22 (81)	10 (77)	0.01 [†]	0.01 [†]
Cord blood (pH) (mean±SD)	7.4±0.04	6.8±0.05	6.9±0.06	0.009 [†]	0.01 [†]

ECMO, extracorporeal membrane oxygenation; HIE, hypoxic-ischemic encephalopathy.

[†]Statistical difference.

Fig. 1

Selected regions (red) overlaid on the mean FA skeleton (white) without a color scale showing the P-value. (a) IFO, (b) ILF, (c) coronal, and (d) axial view at the level of the anterior commissure, (e) GCC, (f) SCC, (g) left and (h) right ALIC, (i) left and (j) right PLIC, (k) left and (l) right SLF, and (m) left and (n) right CS. ALIC, anterior limb of the internal capsule; CS, centrum semiovale; FA, fractional anisotropy; GCC, genu of the corpus callosum; IFO, inferior fronto-occipital fasciculus; ILF, inferior longitudinal fasciculus; PLIC, posterior limb of the internal capsule; SCC, splenium of the corpus callosum; SLF, superior longitudinal fasciculus.

DTI include anisotropy and diffusivity, which are related to the magnitude and direction of physiologic water diffusion within the WM [11]. The sensitivity and specificity of DTI may be enhanced by measuring the individual diffusivities that determine fractional anisotropy (FA), axial diffusivity (AD), and radial diffusivity (RD) [12]. DTI provides clinical or prognostic information for at-risk neonates with HIE or survivors of ECMO for intrinsic lung disease not related to CDH or CHD.

The purpose of this study was therefore to explore the sensitivity of DTI in differentiating putatively normal age-matched infants from survivors of neonatal HIE and ECMO for severe respiratory failure.

Patients and methods

Patients

This study was approved by the institutional review board with written informed parental consent before scanning. Controls [$n=35$, gestational age (GA) 36–42 weeks; mean±SD=39.0±2.6 weeks], HIE patients

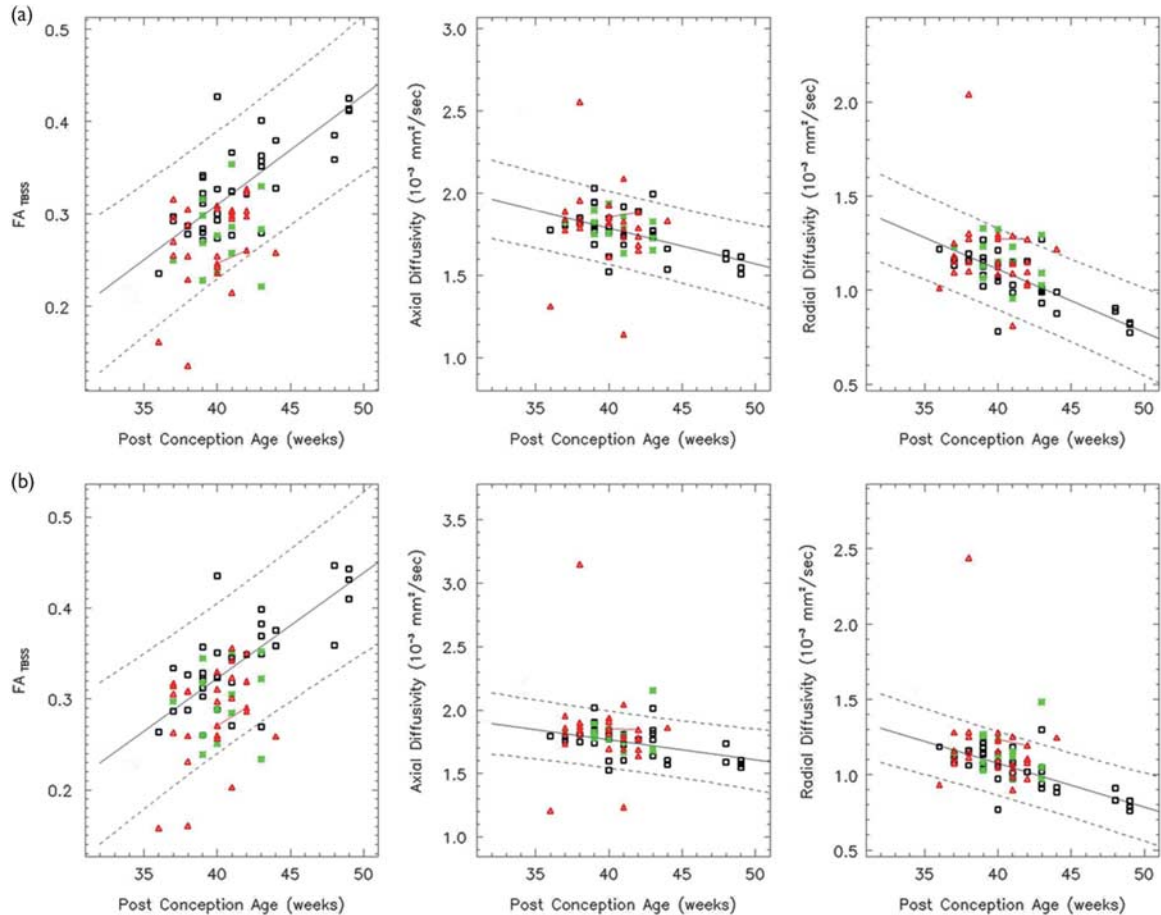
($n=27$, GA 36–41 weeks; mean±SD=38.5±2.5 weeks), and ECMO patients ($n=13$, GA 37–41 weeks; mean±SD=39.0±2.4 weeks) were examined. Patients were recruited from 2013 to 2015. Both HIE and ECMO patients were eligible if they had an Apgar score of less than 5 at both 1 and 5 min after birth, or umbilical cord, arterial, or capillary pH of less than 7.0 or base deficit of at least 16 mM within 1 h after birth [13]. The neonates requiring sedation were sedated with oral chloral hydrate (25–50 mg/kg) before MRI scanning and pulse oximetry; ECG data were monitored, and noise was dampened using earplugs and/or earmuffs for ear protection. All of the examinations were performed under the supervision of a neonatologist experienced in MRI procedures. To minimize selection bias, all neonates during this period of time, in whom the cMRI and DTI were of diagnostic quality, were considered for inclusion in the study on the basis of the following criteria. Patients were categorized as ‘controls’ if (a) they were referred for apnea, bradycardia, or possible congenital intracranial abnormalities in

Table 2 Neurodevelopmental outcomes

DQ (mean ± SD)	Control group (N=33)	HIE group (N=24)	ECMO group (N=13)	P-value control vs. HIE	P-value control vs. ECMO
Total	122.4 ± 11.2	87.6 ± 15.8	88.4 ± 17.8	0.008 [†]	0.02 [†]
Motor	116.8 ± 10.1	92.1 ± 18.8	93.6 ± 20.3	0.09	0.04 [†]
Personal-social	124.3 ± 11.3	89.8 ± 18.4	90.2 ± 18.6	0.006 [†]	0.01 [†]
Hearing and language	122.8 ± 12.6	84.4 ± 22.2	84.4 ± 20.2	0.01 [†]	0.008 [†]
Eye and hand coordination	119.4 ± 10.5	82.3 ± 14.6	84.2 ± 14.8	0.006 [†]	0.008 [†]
Performance	128.6 ± 11.4	84.6 ± 15.4	84.8 ± 16.6	0.005 [†]	0.01 [†]

DQ, development quotient; ECMO, extracorporeal membrane oxygenation; HIE, hypoxic-ischemic encephalopathy.

[†]Statistical difference.

Fig. 2

Both the left (a) and right (b) IFO show a linear increase in the FA over the age range studied (white: controls, red: HIE patients, and green: ECMO patients). Solid lines indicate the mean FA, AD, and RD as determined by a linear regression analysis. Dotted lines indicate 95% confidence intervals. Both the AD and RD decrease linearly. The red line connects a HIE patient imaged longitudinally. In all, 86% of the HIE patients and 93% of the ECMO patients have FA values within the 95% confidence intervals. AD, axial diffusivity; ECMO, extracorporeal membrane oxygenation; FA, fractional anisotropy; HIE, hypoxic-ischemic encephalopathy; IFO, inferior fronto-occipital fasciculus; RD, radial diffusivity.

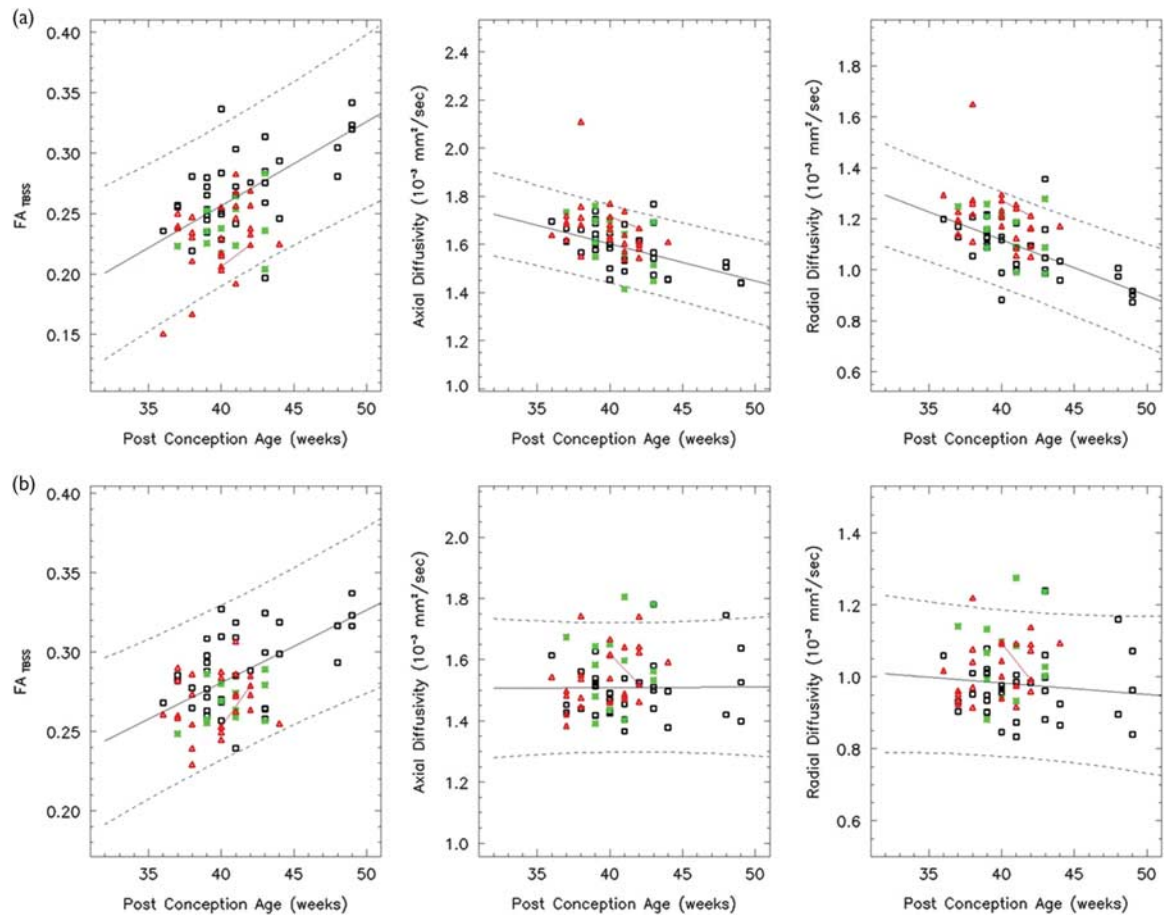
the first 2 weeks of life in the absence of HIE, CHD or CDH, and respiratory failure; (b) cMRI was normal; and (c) the medical records did not document neurologic, motor, or developmental problems either at the time of MRI or at a clinical follow-up. The HIE and ECMO patients underwent MRI as part of their clinical care at our institution. Patients with clinical suspicion of prenatal insults and chromosomal abnormalities were excluded, as

were patients in whom the cMRI showed hydrocephalus or congenital malformations.

Clinical measurements

There were 51 controls initially included in this study. However, 16 patients had epilepsy or neurodevelopmental or motor problems as documented in their medical records during follow-up at a median (range) age of 20

Fig. 3



In the right ILF (a), FA increases linearly over the age range studied (white: controls, red: HIE patients, and green: ECMO patients). Both the AD and RD decrease linearly. In all, 89% of the HIE patients and 93% of the ECMO patients have FA values within the 95% confidence intervals. In the AC (b), the FA increases linearly, but there are no statistically significant age effects on the AD and RD ($F > 0.05$). AC, anterior commissure; AD, axial diffusivity; ECMO, extracorporeal membrane oxygenation; FA, fractional anisotropy; HIE, hypoxic-ischemic encephalopathy; IFO, inferior fronto-occipital fasciculus; ILF, inferior longitudinal fasciculus; RD, radial diffusivity.

(18–21) months, and were therefore excluded from this study. The remaining 35 control patients, who had been born at 36–42 weeks GA, were 36–49 weeks post-conceptual age (PCA) at the time of the MRI (mean \pm SD = 42.6 \pm 4.8 weeks).

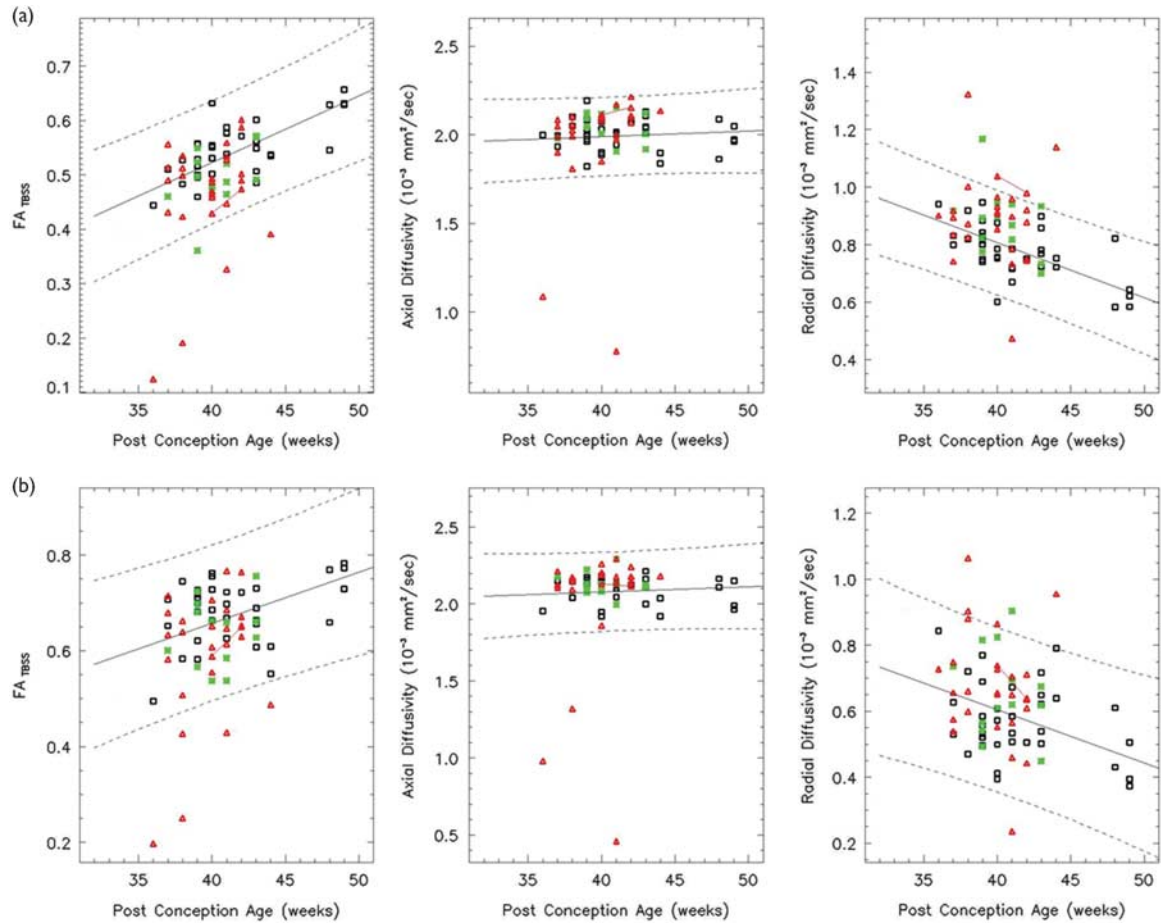
Of 41 HIE patients recruited, 14 patients were excluded because they were suggestive of a chromosomal anomaly or syndromes involving brain dysgenesis or required surgery. The remaining 27 HIE patients, who had been born at 36–41 weeks GA, ranged in PCA from 36 to 44 weeks at the time of the MRI (mean \pm SD = 39.8 \pm 3.4 weeks). The 27 HIE patients underwent therapeutic hypothermia for moderate–severe HIE according to the neonatal research network whole-body cooling protocol with cooling commencing within 6 h after birth [14]. Sarnat grading scores of the cooled neonates were two in 12 patients (moderate HIE) and three in 15 patients (severe HIE).

Fifteen patients underwent ECMO; two were subsequently excluded because of Down's syndrome. GA at birth ranged from 37 to 41 weeks and PCA at the time of MRI ranged from 37 to 43 weeks (mean \pm SD = 40.2 \pm 2.7 weeks). Indications for ECMO were meconium aspiration in three, sepsis in none, and idiopathic persistent pulmonary hypertension in ten. ECMO cannulas were inserted into the right internal jugular vein and the right internal carotid artery in all patients with ligation of the vessels at the time of the cessation of ECMO. Of the 13 patients, two underwent cooling before ECMO. Table 1 shows the baseline characteristics of the infants.

Imaging protocol

MRI was performed on a 3 T Siemens Trio Tim Whole-Body MRI system (Siemens Medical Solution, Erlangen, Germany) using a 12-channel head coil array. cMRI consisted of sagittal and axial T1-weighted FLAIR

Fig. 4



Both the GCC (a) and SCC (b) show a linear increase in the FA over the age range studied (white: controls, red: HIE patients, and green: ECMO patients). The RD decreases linearly, but there is no significant age effect on the AD ($F > 0.05$). In the GCC, 86% of the HIE patients and 93% of the ECMO patients have FA values within the 95% confidence intervals. AD, axial diffusivity; ECMO, extracorporeal membrane oxygenation; FA, fractional anisotropy; GCC, genu of the corpus callosum; HIE, hypoxic-ischemic encephalopathy; RD, radial diffusivity; SCC, splenium of the corpus callosum.

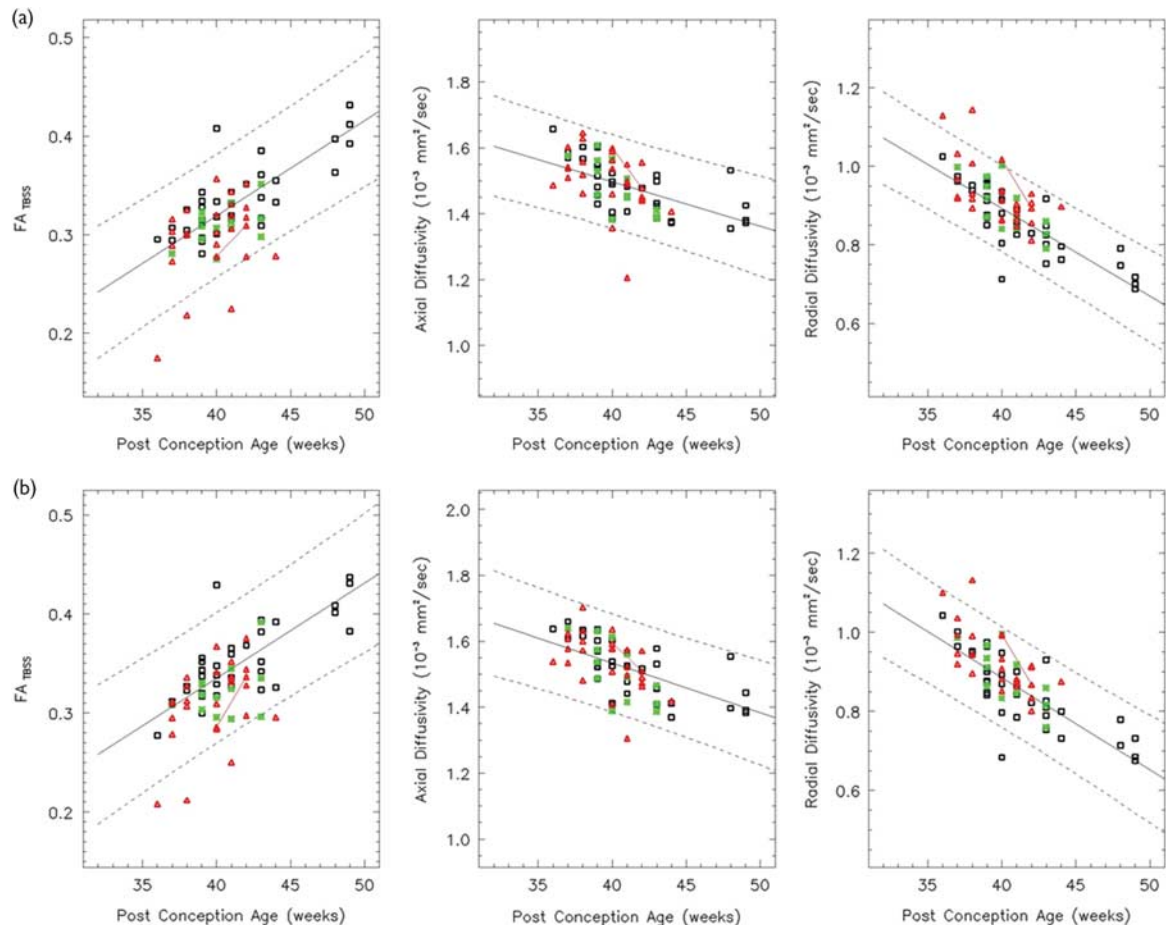
imaging; Echo time (TE)/Inversion time(TI)/Repetition time (TR)=33/1000/2000 ms, $20 \times 20 \text{ cm}^2$ field of view, 200×168 matrix size, $1.0 \times 1.2 \times 3.0 \text{ mm}^3$ voxel size, no gap between slices; axial spin echo T2-weighted imaging; TR/TE = 3000/80 ms, $20 \times 20 \text{ cm}^2$, 200×200 matrix size, 3 mm slice thickness, no gap between slices. DTI was acquired using single-shot Echo-planar imaging (EPI); TE/TR = 74/8000 ms, $20 \times 20 \text{ cm}^2$ field of view, $b = 700 \text{ s/mm}^2$, 128×128 matrix size, $1.6 \times 1.6 \times 2.0 \text{ mm}^3$ voxel size, SENSE factor=2, and 30 gradient directions [15]. The geometry accuracy of the MRI scanner, including high-contrast resolution, low-contrast detectability, and B_0 shifting, was checked weekly over the period of the image review following our local quality assurance protocol. The signal-to-noise ratio (SNR) of the tensor data was analyzed to document the American College of Radiology (ACR) phantom SNR using the DTI quality assurance analysis tool provided by the Siemens system and a method described previously [16].

Neurodevelopmental assessment and image analysis

Most of the study patients were brought to the follow-up, and neurodevelopmental outcomes were assessed by pediatricians performing the Griffiths Mental Development Scales (revised) testing [17]. Five subscales (locomotor, personal-social, hearing and language, eye and hand coordination, and performance) of development were evaluated [18].

All conventional MRI studies were retrospectively reviewed by an experienced pediatric neuroradiologist with 30 years of experience. If any abnormality was questionable by the cMRI upon a retrospective review of the controls, the case was excluded. Consensus was reached on the cMRI findings for the HIE and ECMO patients. For the HIE patients, images were graded as abnormal when showing a basal ganglia/thalamus pattern of injury, a watershed injury pattern, or mixed. On the basis of previous reports of cMRI findings in survivors of neonatal ECMO, [18] the MRI results of the ECMO survivors were graded as normal when showing either

Fig. 5



Both the left (a) and right (b) ALIC show a linear increase in the FA over the age range studied (white: controls, red: HIE patients, and green: ECMO patients). Both the AD and RD decrease linearly. In all, 86% of the HIE patients and 93% of the ECMO patients have FA values within the 95% confidence intervals. AD, axial diffusivity; ALIC, anterior limb of the internal capsule; ECMO, extracorporeal membrane oxygenation; FA, fractional anisotropy; HIE, hypoxic-ischemic encephalopathy; RD, radial diffusivity.

expanded cerebrospinal fluid (CSF) spaces in the absence of signal abnormalities in the brain or expanded CSF spaces with parenchymal signal abnormalities.

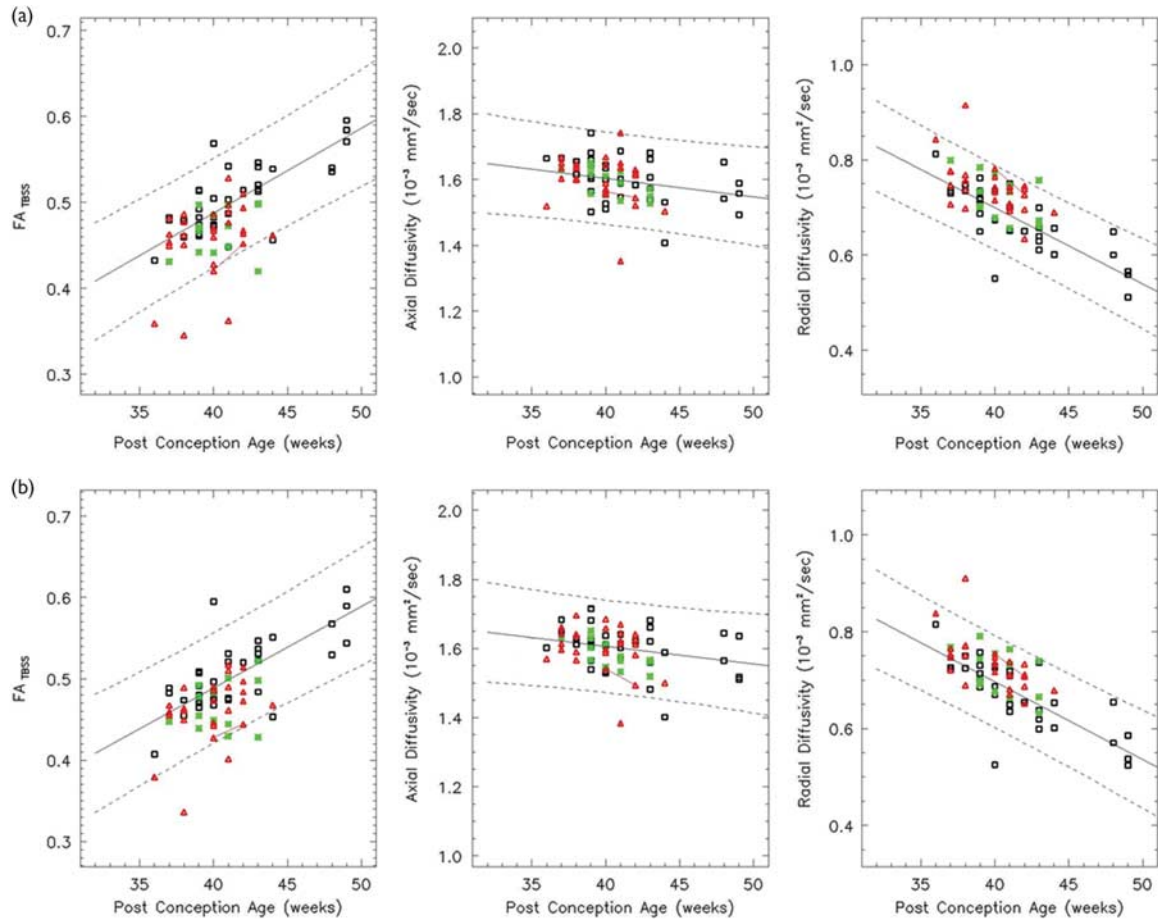
Image processing

The individual DTI data were registered and averaged off-line using DTI Studio [19] with affine transformation for the correction of eddy current distortion and head motions. The SNR (≥ 26) of each patient data set was assessed at the genu of the corpus callosum, and all data were found to exceed the SNR threshold ($= 20$) for bias-free FA measurements [20].

FSL (FMRIB Software Library; FMRIB, Oxford, UK) [21,22] was used to acquire the diffusion tensor eigenvectors and eigenvalues and to generate the FA images with Tract-Based Spatial Statistics (TBSS) modified for use in infants [23,24]. A target image was calculated from the mean intensity of all aligned FA images and used as

the reference for a second iteration of the rigid, affine, and nonlinear registration of each patient's FA map. The mean displacement score for all potential targets ranged from 1.52 to 4.78 (median 2.93). The target patient was a 40-week girl with a minimum mean displacement score of 1.52; transformation to a standard adult space was not performed. The mean FA image was used to create a mean FA skeleton (FA threshold = 0.15). The FA data from each patient were projected onto the mean FA skeleton. To obtain AD and RD data, the principal eigenvalues were projected onto the mean FA skeleton. The modified TBSS outcomes were plotted and analyzed using custom software written in IDL 8.2 (IDL Research Systems Inc., Boulder, Colorado, USA) by a single experienced observer who manually placed regions of interest in 9 regions: the inferior fronto-occipital fasciculus (IFO), inferior longitudinal fasciculus (ILF), anterior commissure (AC), genu (GCC) and splenium (SCC) of the corpus callosum, anterior limb of internal capsule (ALIC)

Fig. 6



Both the left (a) and right (b) PLIC show a linear increase in the FA and a linear decrease in the RD over the age range studied (white: controls, red: HIE patients, and green: ECMO patients). The left PLIC shows a linear decrease in the AD, but the right PLIC does not ($F > 0.05$). In all, 86% of the HIE patients and the ECMO patients have FA values within the 95% confidence intervals. AD, axial diffusivity; ECMO, extracorporeal membrane oxygenation; FA, fractional anisotropy; HIE, hypoxic-ischemic encephalopathy; PLIC, posterior limb of the internal capsule; RD, radial diffusivity.

and posterior limb of internal capsule (PLIC), superior longitudinal fasciculus (SLF), and the centrum semiovale (CS) (Fig. 1). Tensor metrics of the selected regions of the brain were averaged over 11 contiguous voxels on the mean FA skeleton.

Statistical analysis

Linear regression analysis was performed for age effects on the FA, AD, and RD using the only control cohort; 95% confidence intervals (CIs) ($= 1.96 \times \text{SD}$ below and above the mean) were also created using the control tensor data. Patients whose FA, AD, and/or RD values fell outside the 95% CIs were identified as abnormal by DTI. Both r and significance F -values were calculated to check whether the regression models for the tensor metrics in the selected regions of the brain would be good fits (significance if $F < 0.05$). Two-sample t -test was done to determine whether there was a difference in the mean FA, AD, RD, and neurodevelopmental outcomes

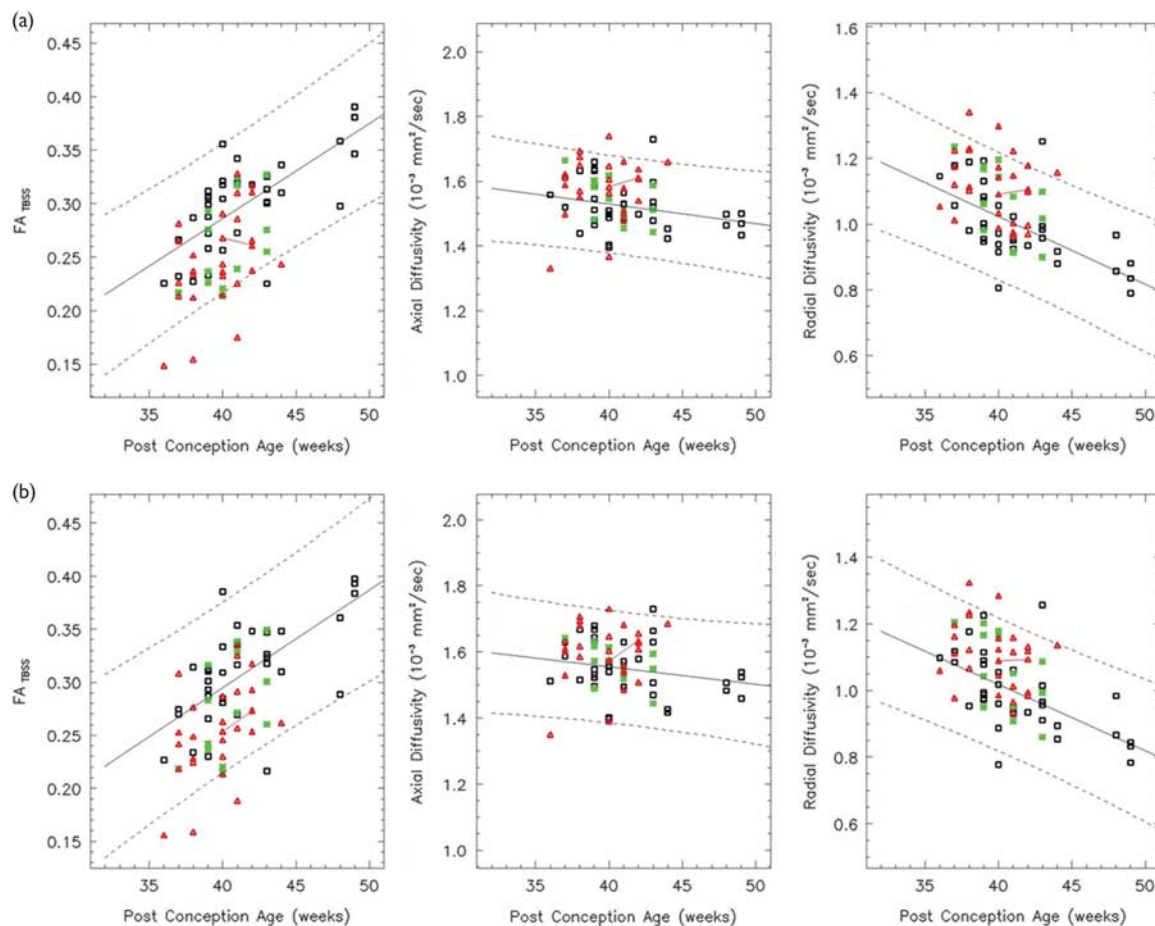
between the normal and HIE, and the normal and ECMO cohorts. Data were considered significant at a two-tailed P value less than 0.05; statistical calculations were done with SPSS, version 16.0 (SPSS Inc., Chicago, Illinois, USA).

Results

Follow-up clinical examination

Of the 35 control patients, two were lost to follow-up. Thirty-three were assessed at the follow-up ranging from 19 to 21 months; 3/33 (9%) had motor or developmental problems. 30/33 (91%) were normal. Of the 27 survivors of HIE, three were lost to follow-up. 18/24 (75%) were normal, and 6/24 (25%) had an abnormal tone, motor problems, or developmental delay. Of the 13 ECMO survivors, three required prolonged enteric feeding, including gastrostomy tubes in two; however, it was documented that they had normal oral intake by 18 months of age. Seven of the 13 ECMO survivors had a normal neuromotor

Fig. 7



In the left (a) and right (b) SLF, the FA increases linearly over the age range studied (white: controls, red: HIE patients, and green: ECMO patients). Both the AD and RD decrease linearly. In all, 86% of the HIE patients and 100% of the ECMO patients have FA values within the 95% confidence intervals. AD, axial diffusivity; ECMO, extracorporeal membrane oxygenation; FA, fractional anisotropy; HIE, hypoxic-ischemic encephalopathy; RD, radial diffusivity; SLF, superior longitudinal fasciculus.

outcome, and six were developmentally delayed at the follow-up.

Conventional MRI outcomes

By definition, the cMRI was normal in all control patients. Of the 27 HIE patients, 74% ($n=20$) of the HIE patients had a normal cMRI. Among the seven HIE patients with an abnormal cMRI, there was basal ganglia or thalamus injury in two patients and watershed injury without basal ganglia or thalamus injury in another two patients, and three patients showed WM abnormalities and hypo-intensities in the callosal genu or splenium. Of the 13 ECMO patients, eight (62%) had a normal cMRI without expansion of the CSF spaces, and three had expanded CSF spaces with prominent ventricles. Two patients had small cortical infarcts in the left occipital WM and right temporal WM.

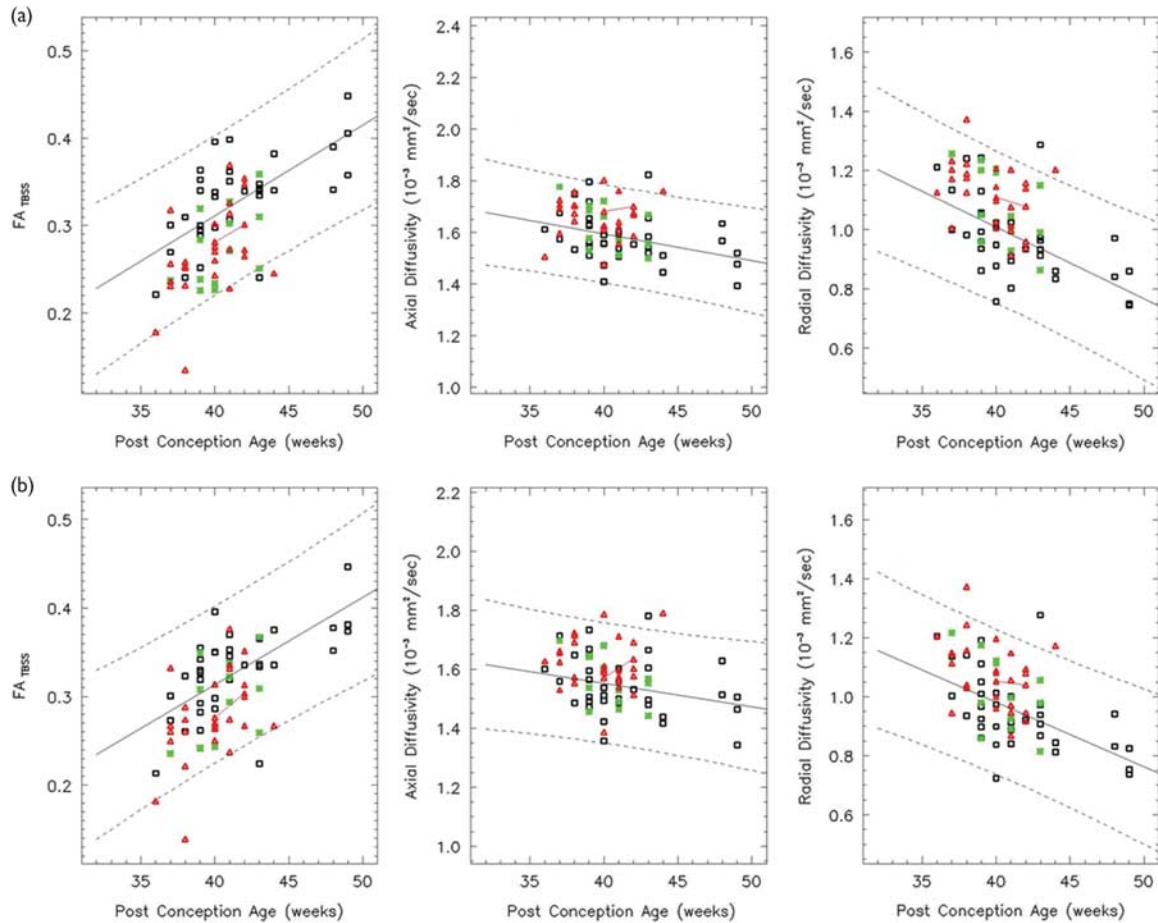
Neurodevelopmental outcomes

Mean global development quotients and quotients for all the individual subscales were higher in the control group than in both HIE and ECMO groups (Table 2). Significant differences were found in total development quotients, social, hearing and language, eye and hand coordination, and performance subscales between the normal and patient cohort except motor subscale between the normal and HIE cohort.

Age-related changes in tensor metrics and group comparisons

Age-related changes in the mean FA, AD, and RD values in the selected regions of the brain are shown in Figs 2–8. Descriptive statistical outcomes are summarized in Table 3. The regression models for the tensor metrics showed good fits in most regions except for the axial and radial diffusivities in the AC, and the axial diffusivity in the GCC, right PLIC, and SCC ($F > 0.05$). In our control

Fig. 8



Both the left (a) and right (b) CS show a linear increase in the FA and both the AD and RD decrease linearly over the age range studied (white: controls, red: HIE patients, and green: ECMO patients). In all, 89% of HIE patients and the ECMO patients have FA values within the 95% confidence intervals. AD, axial diffusivity; CS, centrum semiovale; ECMO, extracorporeal membrane oxygenation; FA, fractional anisotropy; HIE, hypoxic-ischemic encephalopathy; RD, radial diffusivity.

patients, age-related increases in the FA in the AC, GCC, right PLIC, and SCC stemmed from the decreased RD in the absence of changes in the AD, whereas in the other regions of the brain age-related FA increases were associated with decreases in both the AD and RD. Two controls, four HIE, and two ECMO patients were outside the 95% CIs of FA, AD, and/or RD in most regions.

A group difference in the FA and RD between the normal and HIE was seen in the anatomical regions selected in this study ($P < 0.05$). A group difference in the FA and RD between the control and ECMO is seen in the AC, CS bilaterally, GCC, IFO bilaterally, right ILF, and SLF bilaterally ($P < 0.05$).

Discussion

At our institution, DTI is a routine sequence, although one acquisition adds 3–4 min to the acquisition time. For the purpose of this study, the tensor data were post-processed off-line, requiring hardware, software, and

trained personnel. We sought to determine whether DTI acquired in the neonatal period in a routine clinical setting could differentiate between the control and patient populations.

The reliability of DTI measures calculated by the standard TBSS approach in normal adult patients was affected by different processing pipeline choices [25]. In this study, voxel-wise processing of the tensor data was performed using an optimized protocol, which we have modified to improve the reliability in neonatal DTI analysis.

Previous study [26] demonstrated that mean diffusivity significantly decreased in many regions of white and gray matter. In this study, we observed that FA increased and RD decreased in the selected regions showing age effects on the FA and RD in this neonatal period. Our results suggest that age-related changes in the FA and RD correlate with differences in the WM FA and RD between

Table 3 Statistical outcomes in the selected regions of the brain

Locations	Tensor metrics	Regression analysis ($F < 0.05$, significance)		Two-sample <i>t</i> -test ($P < 0.05$, significance)		
		<i>r</i>	<i>F</i> -value	Normal vs. HIE (<i>P</i> -value)	Normal vs. ECMO (<i>P</i> -value)	
AC	FA	0.71	0.001	0.002 [†]	0.003 [†]	
	AD	0.04	0.926	0.198	0.043 [†]	
	RD	0.13	0.255	0.042 [†]	0.011 [†]	
ALIC	Left	FA	0.73	0.001	0.002 [†]	0.033 [†]
		AD	0.68	0.002	0.213	0.878
		RD	0.75	0.001	0.004 [†]	0.192
	Right	FA	0.69	0.002	0.001 [†]	0.067
		AD	0.48	0.004	0.295	0.704
		RD	0.75	0.001	0.002 [†]	0.201
CS	Left	FA	0.71	0.001	0.001 [†]	0.005 [†]
		AD	0.49	0.006	0.003 [†]	0.089
		RD	0.70	0.003	0.002 [†]	0.013 [†]
	Right	FA	0.70	0.002	0.002 [†]	0.008 [†]
		AD	0.47	0.008	0.003 [†]	0.256
		RD	0.61	0.006	0.002 [†]	0.036 [†]
GCC	FA	0.77	0.001	0.001 [†]	0.019 [†]	
	AD	0.07	0.526	0.681	0.108	
	RD	0.73	0.002	0.001 [†]	0.008 [†]	
IFO	Left	FA	0.73	0.001	0.001 [†]	0.006 [†]
		AD	0.42	0.008	0.204	0.169
		RD	0.67	0.003	0.006 [†]	0.029 [†]
	Right	FA	0.67	0.003	0.003 [†]	0.004 [†]
		AD	0.28	0.012	0.113	0.071
		RD	0.49	0.009	0.004 [†]	0.011 [†]
Right ILF	FA	0.64	0.006	0.002 [†]	0.002 [†]	
	AD	0.57	0.007	0.004 [†]	0.121	
	RD	0.65	0.004	0.001 [†]	0.031 [†]	
PLIC	Left	FA	0.70	0.002	0.001 [†]	0.033 [†]
		AD	0.26	0.018	0.759	0.574
		RD	0.71	0.001	0.001 [†]	0.077
	Right	FA	0.66	0.004	0.001 [†]	0.032 [†]
		AD	0.21	0.063	0.959	0.263
		RD	0.73	0.002	0.001 [†]	0.101
SLF	Left	FA	0.65	0.003	0.001 [†]	0.013 [†]
		AD	0.29	0.009	0.003 [†]	0.162
		RD	0.68	0.004	0.002 [†]	0.033 [†]
	Right	FA	0.66	0.004	0.004 [†]	0.028 [†]
		AD	0.27	0.015	0.024 [†]	0.276
		RD	0.61	0.009	0.004 [†]	0.047 [†]
SCC	FA	0.52	0.008	0.003 [†]	0.172	
	AD	0.08	0.505	0.387	0.187	
	RD	0.52	0.007	0.014 [†]	0.068	

AC, anterior commissure; AD, axial diffusivity; ALIC, anterior limb of internal capsule; CS, centrum semiovale; FA, fractional anisotropy; GCC, genu of the corpus callosum; IFO, inferior fronto-occipital fasciculus; ILF, inferior longitudinal fasciculus; PLIC, posterior limb of internal capsule; RD, radial diffusivity; SCC, splenium of the corpus callosum; SLF, superior longitudinal fasciculus.

[†]Statistical difference.

age-equivalent putatively normal control patients and encephalopathic neonates of HIE and ECMO with the exception of the radial diffusivity in the left ALIC and PLIC bilaterally, and the fractional anisotropy and radial diffusivity in the right ALIC and SCC between the normal and ECMO cohort. However, age-related changes in the AD are less associated with differences in the axial diffusivity between the normal and patient cohort. Significant DTI comparisons among the groups were

found possibly because of the DTI acquisition occurring soon after the time of the insult, suggesting that the hypoxic–ischemic insult affected the microstructure of immature axons. FA and RD are suitable biomarkers for the evaluation of microstructural damage to WM structures. The age-related changes in the FA and RD suggest that neonatal patients should be matched to controls of the same or similar PCA.

The same patients were outliers in most regions, which might be expected for a global insult. Four HIE patients and one survivor of ECMO who were outside the 95% CIs of the FA, AD, and RD overlapped with those with abnormalities clinically and on the cMRI. In addition, two normal patients were outliers with poor clinical outcomes. DTI acquired during the neonatal period could differentiate between typical developing patients and those with documented neurodevelopmental problems in the selected regions of the brain.

A previous study [18] demonstrated that TBSS could be used as an independent, objective, and sensitive method for tensor data analysis to reveal multiple WM microstructural abnormalities in several WM tracts in HIE neonatal brains. However, our present results indicated that impaired WM tracts were associated with widespread WM abnormalities in neonates with ECMO, as well as HIE. In our populations of patients, determination of the diffusivities did improve the accuracy of DTI.

A limitation of this study is the lack of documentation of normal neurodevelopmental status in the control patients; in some control patients, follow-up at our institution was limited to visits to the emergency room for minor medical problems. However, many of the patients included in the control cohort had been referred from a geographically ‘normal’ cohort. We did not include a neurological examination at the time of discharge because the predictive value of a normal neonatal neurologic examination is fairly limited, and concluding that survivors of HIE will be neurodevelopmentally normal based on a clinical evaluation is problematic.

Conclusion

DTI can play a significant role in detecting patients with poor clinical outcomes and with abnormalities on cMRI for the early detection of certain pathologies in this population.

Acknowledgements

This work was funded by the National Research Foundation of Korea (NRF-2014R1A1A2054037).

Conflicts of interest

There are no conflicts of interest.

References

- 1 Albertine KH. Brain injury in chronically ventilated preterm neonates: collateral damage related to ventilation strategy. *Clin perinatol* 2012; **39**:727–740.
- 2 Laptook AR. Use of therapeutic hypothermia for term infants with hypoxic–ischemic encephalopathy. *Pediatr Clin North Am* 2009; **56**:601–616.
- 3 Huang BY, Castillo M. Hypoxic–ischemic brain injury: imaging findings from birth to adulthood. *Radiographics* 2008; **28**:417–439.
- 4 Bulas D, Glass P. Neonatal ECMO: neuroimaging and neurodevelopmental outcome. *Semin Perinatol* 2005; **29**:58–65.
- 5 Shankaran S, Laptook AR, Ehrenkranz RA, Tyson JE, McDonald SA, Donovan EF, et al. Whole-body hypothermia for neonates with hypoxic–ischemic encephalopathy. *N Engl J Med* 2005; **353**:1574–1584.
- 6 Amigoni A, Pettenazzo A, Biban P, Suppiej A, Freato F, Zaramella P, et al. Neurologic outcome in children after extracorporeal membrane oxygenation: prognostic value of diagnostic tests. *Pediatr Neurol* 2005; **32**:173–179.
- 7 Schaible T, Busing KA, Felix JF, Hop WC, Zahn K, Wessel L, et al. Prediction of chronic lung disease, survival and need for ECMO therapy in infants with congenital diaphragmatic hernia: additional value of fetal MRI measurements? *Eur J Radiol* 2012; **81**:1076–1082.
- 8 Hamrick SE, Gremmels DB, Keet CA, Leonard CH, Connell JK, Hawgood S, et al. Neurodevelopmental outcome of infants supported with extracorporeal membrane oxygenation after cardiac surgery. *Pediatrics* 2003; **111**:671–675.
- 9 Glass P, Wagner AE, Papero PH, Rajasingham SR, Civitello LA, Kjaer MS, et al. Neurodevelopmental status at age five years of neonates treated with extracorporeal membrane oxygenation. *J Pediatr* 1995; **127**:447–457.
- 10 Bassler PJ. Inferring microstructural features and the physiological state of tissues from diffusion-weighted images. *NMR Biomed* 1995; **8**:333–344.
- 11 Bassler PJ, Pierpaoli C. Microstructural and physiological features of tissues elucidated by quantitative-diffusion-tensor MRI. *J Magn Reson* 1996; **111**:209–219.
- 12 Song SK, Yoshino J, Le TQ, Lin SJ, Sun SW, Cross AH, et al. Demyelination increases radial diffusivity in corpus callosum of mouse brain. *Neuroimage* 2005; **26**:132–140.
- 13 Azzopardi DV, Strohm B, Edwards AD, Dyet L, Halliday HL, Juszczak E, et al. Moderate hypothermia to treat perinatal asphyxial encephalopathy. *N Engl J Med* 2009; **361**:1349–1358.
- 14 Jacobs SE, Berg M, Hunt R, Tarnow-Mordi WO, Inder TE, Davis PG. Cooling for newborns with hypoxic ischaemic encephalopathy. *Cochrane Database Syst Rev* 2013; **1**:CD003311.
- 15 Jones DK, Horsfield MA, Simmons A. Optimal strategies for measuring diffusion in anisotropic systems by magnetic resonance imaging. *Magn Reson Med* 1999; **42**:515–525.
- 16 Wang ZJ, Seo Y, Chia JM, Rollins NK. A quality assurance protocol for diffusion tensor imaging using the head phantom from American College of Radiology. *Med Phys* 2011; **38**:4415–4421.
- 17 Huntley M. *The Griffiths Mental Development Scales: From Birth to 2 years*. Oxford, UK: Association for Research in Infant and Child Development (ARICD); 1996. pp. 5–39.
- 18 Tumor N, Wusthoff C, Smeets N, Merchant N, Arichi T, Allsop JM, et al. Prediction of neurodevelopmental outcome after hypoxic-ischemic encephalopathy treated with hypothermia by diffusion tensor imaging analyzed using tract-based spatial statistics. *Pediatr Res* 2012; **72**:63–69.
- 19 Jiang H, van Zijl PC, Kim J, Pearlson GD, Mori S. DtiStudio: resource program for diffusion tensor computation and fiber bundle tracking. *Comput Methods Programs Biomed* 2006; **81**:106–116.
- 20 Seo Y, Wang ZJ, Morriss MC, Rollins NK. Minimum SNR and acquisition for bias-free estimation of fractional anisotropy in diffusion tensor imaging – a comparison of two analytical techniques and field strengths. *Magn Reson Imaging* 2012; **30**:1123–1133.
- 21 Smith SM, Jenkinson M, Woolrich MW, Beckmann CF, Behrens TE, Johansen-Berg H, et al. Advances in functional and structural MR image analysis and implementation as FSL. *Neuroimage* 2004; **23** (Suppl 1): 208–219.
- 22 Woolrich MW, Jbabdi S, Patenaude B, Chappell M, Makni S, Behrens T, et al. Bayesian analysis of neuroimaging data in FSL. *Neuroimage* 2009; **45**:173–186.
- 23 Ball G, Counsell SJ, Anjari M, Merchant N, Arichi T, Doria V, et al. An optimised tract-based spatial statistics protocol for neonates: applications to prematurity and chronic lung disease. *Neuroimage* 2010; **53**:94–102.
- 24 Seo Y, Wang ZJ, Ball G, Rollins NK. Diffusion tensor imaging metrics in neonates—a comparison of manual region-of-interest analysis vs. tract-based spatial statistics. *Pediatr Radiol* 2013; **43**:69–79.
- 25 Madhyastha T, Merillat S, Hirsiger S, Bezzola L, Liem F, Grabowski T, et al. Longitudinal reliability of tract-based spatial statistics in diffusion tensor imaging. *Hum Brain Mapp* 2014; **35**:4544–4555.
- 26 Ancora G, Testa C, Grandi S, Tonon C, Sbravati F, Savini S, et al. Prognostic value of brain proton MR spectroscopy and diffusion tensor imaging in newborns with hypoxic–ischemic encephalopathy treated by brain cooling. *Neuroradiology* 2013; **55**:1017–1025.